

# FORMATION TETRAHEDRON DESIGN FOR PHASE I OF THE MAGNETOSPHERIC MULTISCALE MISSION

Steven P. Hughes

Flight Dynamics Analysis Branch  
NASA Goddard Space Flight Center

## ABSTRACT

The Magnetospheric Multiscale Mission (MMS) is a NASA mission intended to make fundamental advancements in our understanding of the Earth's Magnetosphere. There are three processes that MMS will study including magnetic reconnection, charged particle acceleration, and turbulence.<sup>1</sup> There are four phases in the nominal mission and this work addresses some of the outstanding issues in phase I. The nominal phase I orbit is a  $1.2 \times 12 R_e$  highly elliptic orbit with four spacecraft nominally forming a regular tetrahedron. In this paper we investigate the relative dynamics of the four MMS spacecraft about an assumed reference orbit. There are several tetrahedron dimensions required in Phase I of the mission and in this work we design optimal tetrahedrons for the 10 km baseline. The performance metric used in the optimization process is directly related to the science return, and is based on an extension of previous work performed by Glassmeier.<sup>2</sup> The optimizer we use is a commercially available Sequential Quadratic Programming (SQP) routine. Multiple optimal solutions are found, and we characterize how the performance of the formation varies between different regions of the reference orbit.

## INTRODUCTION

The MMS mission is one of several missions in NASA's Solar Terrestrial Probe (STP) program. The goal of MMS is to make fundamental advancements in our understanding of the Earth's magnetosphere and its dynamic interaction with the solar wind. Previous research has been limited due to the reliance on single-spacecraft measurements which are not adequate to reveal the underlying physics of highly dynamic, highly structured plasma processes. By taking advantage of the latest multi-spacecraft mission technology, MMS will be able to differentiate between spatial and temporal effects and to determine the three-dimensional geometry of the plasma, field, and current structures under study.<sup>1</sup>

The nominal orbital configuration of the four spacecraft is a regular tetrahedron and the size of the tetrahedron is to be varied to allow insight into the different scales at which plasma processes occur. The reference orbit for phase I is nominally a  $1.2 \times 12 R_e$  Highly Elliptic Orbit (HEO), but detailed phase I reference orbit design is a topic of current and future research. The orbit design work presented here only addresses the tetrahedron design for phase I. Ideally the spacecraft should maintain a regular tetrahedron for the entire orbit. However, this is not possible within the constraints of Keplerian dynamics, and active control is prohibitively expensive. Our goal in this

work is to quantify the level of performance that we can provide using Keplerian orbits. Orbits that perform well yield a large quantity of useful science data, and orbits that perform poorly yield less useful science data. As the shape of the tetrahedron evolves over an orbit, the ability of the configuration to provide adequate science return will vary. It is important to note that a regular tetrahedron need not ever be actually achieved; however, it is desirable that the geometries are as near regular as possible. With this work we wish to determine how long we can maintain useful tetrahedron configurations, and determine what parts of the orbit near-regular tetrahedrons can be maintained for the longest duration.

Our approach to the formation design is to develop a performance metric that is related to the science return provided by a particular formation configuration, and then use Sequential Quadratic Programming (SQP) to find optimal solutions. We begin by developing a function that allows a measure of performance for a given formation at a particular instant. Then we formulate a composite metric that provides a performance measure over different regions of interest along the reference orbit. The instantaneous metric is formulated to reflect both the quality of the shape of the tetrahedron, as well as the size of the tetrahedron. We parameterize the performance metric in terms of the orbital elements, where all orbits have a common semimajor axis to ensure equal periods. Bound constraints are applied to ensure that the solutions are in the vicinity of the current nominal reference orbit for phase I.

Multiple solutions are presented for optimal tetrahedron configurations. The solutions are generated by optimizing over different regions of the reference orbit. The regions of interest are defined by two variables. The first is the reference true anomaly,  $\nu_c$ , that defines the center of the region of interest. The second independent variable is the width of the region of interest, in terms of a change in true anomaly  $\Delta\nu$ . For example, one optimal solution is centered at a true anomaly of 180 so  $\nu_c = 180$ , and the width of the region of interest is 60 degrees, so  $\Delta\nu = 60$ . Several solutions are presented in detail to illustrate the nature of the results found using the approach developed in this work. Secondly, a contour plot of the orbit performance vs  $\nu_c$  and  $\Delta\nu$  is presented to enable some general conclusions about which parts of the orbit we can provide the best science return, and how long we can realistically maintain useful tetrahedron geometries.

## ORBIT DESIGN

The orbit design for phase I of the MMS mission can be broken down into two parts. One part is designing the optimal reference orbit. The second part is designing the optimal relative motion about the reference. In this work we only focus on designing formations that provide optimal relative motion between the four spacecraft. Optimal reference orbit design is a topic of current and future research. To maximize science return it is desirable to maintain a regular tetrahedron over the entire orbit. However, as previously mentioned, this is not possible using Keplerian orbits and using active control to maintain a regular tetrahedron is prohibitively costly. In this work we design orbits that provide the maximum performance possible with Keplerian orbit dynamics. Our goal is to characterize the performance that we can provide by carefully optimizing the relative motion of the four spacecraft. In general the performance will vary in time and it is important to determine for which regions of the reference orbit we can provide acceptable science return.

In the following few subsections we present the approach used to determine optimal relative motion solutions for phase I of the MMS mission. We begin by discussing basic geometric properties of tetrahedrons, including the surface area and volume. Next we develop an orbit performance metric that is used in the optimization process. The performance metric is directly related to the science return and is an extension of work performed by Glassmeier.<sup>2</sup> We also describe the independent variables chosen for this work and discuss the bound constraints we apply to ensure that the dimensions of the orbit solutions are in the vicinity of the desired reference orbit. We conclude the section with a discussion of an algorithm to provide initial guesses to the optimization process, and the type of numerical optimizer used in this work.

## Tetrahedron Geometry

To provide the maximum science return, the spacecraft should form a regular tetrahedron for the entire orbit. Although this is not physically possible without considerable fuel expenditure, it is useful to discuss some properties of regular tetrahedrons because it is possible to provide near-regular tetrahedron formations for large portions of an orbit by appropriately designing Keplerian orbits. One possible parameterization for a regular tetrahedron is given by

$$\mathbf{d}_1 = (L, 0, 0) \quad (1)$$

$$\mathbf{d}_2 = \left(\frac{L}{2}, \frac{\sqrt{3}L}{2}, 0\right) \quad (2)$$

$$\mathbf{d}_3 = \left(\frac{L}{2}, \frac{\sqrt{3}L}{6}, \frac{\sqrt{6}L}{3}\right) \quad (3)$$

$$\mathbf{d}_4 = (0, 0, 0) \quad (4)$$

where  $L$  is the length of the sides of the tetrahedron. The tetrahedron volume is given by

$$V = \frac{1}{6} \|\mathbf{d}_1 \cdot (\mathbf{d}_2 \times \mathbf{d}_3)\| \quad (5)$$

The tetrahedron surface area is given by

$$S = \frac{1}{2} (\|\mathbf{d}_2 \times \mathbf{d}_3\| + \|\mathbf{d}_1 \times \mathbf{d}_3\| + \|\mathbf{d}_1 \times \mathbf{d}_2\| + \|\mathbf{d}_1 \times \mathbf{d}_2 + \mathbf{d}_2 \times \mathbf{d}_3 + \mathbf{d}_3 \times \mathbf{d}_1\|) \quad (6)$$

The expressions for the volume and area of a tetrahedron will be particularly useful in defining a performance metric in the next section.

## Performance Metrics

Developing a useful performance metric for a mission such as MMS is non-trivial. However, significant work can be found in the literature and Paschmann<sup>2</sup> provides a good review. First we require a measure that allows us to ascertain the science return provided by a particular relative geometry at a given instant. Then, given an instantaneous performance metric we need a way to determine the performance of a particular orbit design over a specific region of interest in the orbit.

There are many different possible formulations for an instantaneous tetrahedron quality metric, and we have chosen one based on work by Glassmeier.<sup>2</sup> Glassmeier's metric is written as

$$Q_{GM} = \frac{V_a}{V^*} + \frac{S_a}{S^*} + 1 \quad (7)$$

where  $V_a$  is the actual volume of a given tetrahedron,  $S_a$  is the actual surface area of a given tetrahedron,  $V^*$  is the volume of a regular tetrahedron with sides equal to the average side length of the actual tetrahedron, and  $S^*$  is the area of a regular tetrahedron with sides equal to the average side length of the actual tetrahedron. It is important to note that the following two relations are always true:

$$V_a \leq V^* \quad (8)$$

and

$$S_a \leq S^* \quad (9)$$

Hence, the maximum value of  $Q_{GM}$  is three and this occurs when the formation is in a regular tetrahedron configuration. The value of  $Q_{GM}$  is one when the formation is collinear, or collocated. Glassmeier's quality metric provides a way of determining the regularity of a tetrahedron. However, it is important to note that it does not give any information about the size of the tetrahedron. All regular tetrahedrons, regardless of the side length  $L$ , have the property  $Q_{GM} = 3$ . This is a concern because the size of the tetrahedron formation is important for MMS.

We propose a modification to Glassmeier's metric to allow it to contain information on not only the tetrahedron shape, but also its size. There are many ways in which we can modify  $Q_{GM}$  to include information on the tetrahedrons size. Before we modify the metric  $Q_{GM}$ , we define a simple function  $S(L^*)$  defined as follows:

$$S(L^*) = \begin{cases} 0 & L^* < \ell_1 \\ (L^* - \ell_1)^2(L^* + \ell_1 - 2\ell_2)^2/(\ell_2 - \ell_1)^4 & \ell_1 < L^* < \ell_2 \\ 1 & \ell_2 < L^* < \ell_3 \\ (L^* - \ell_4)^2(L^* - 2\ell_3 + \ell_4)^2/(\ell_4 - \ell_3)^4 & \ell_3 < L^* < \ell_4 \\ 0 & L^* > \ell_4 \end{cases} \quad (10)$$

where  $L^*$  is the average side length, and  $\ell_1 = 2$ ,  $\ell_2 = 4$ ,  $\ell_3 = 18$ , and  $\ell_4 = 20$ . A graph of  $S(L^*)$  is shown in Figure 1 and provides an intuitive description of the function. Recall that we are interested in providing tetrahedrons with dimensions on the order of 10 km. For this reason, we have designed  $S(L^*)$  to be zero when the average side length is not near 10 km. The limits chosen here are that  $S(L^*)$  is zero for tetrahedrons with average side lengths of less than 2 km, or greater than 20 km.

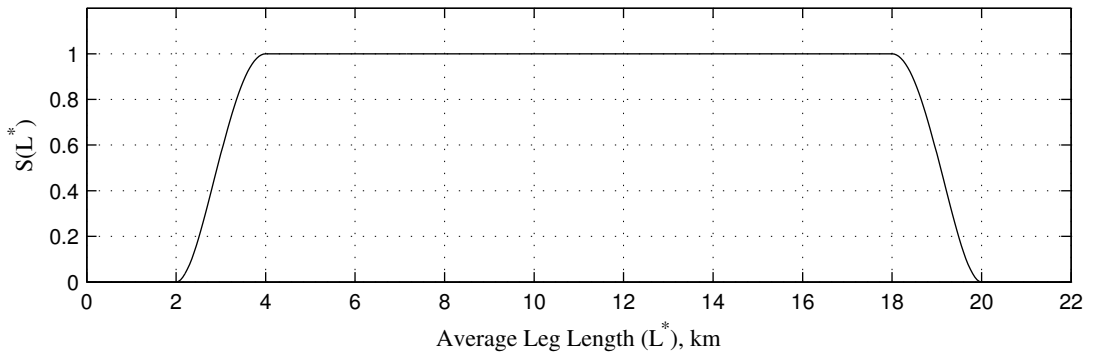


**Figure 1:** Plot of  $S(L^*)$

By posing a composite quality metric  $Q_C$  defined as

$$Q_C = Q_{GM} * S(L^*) \quad (11)$$

we have a metric that contains information on both the size and shape of the tetrahedron. When the value of  $Q_C$  is three, we know that the formation is in a regular tetrahedron configuration, and that the side length is somewhere between 4 and 18 km.

Given an instantaneous measure of performance, we need to formulate a general expression to provide a measure of performance over a region of interest. One possible general expression for a performance metric of this type is

$$J_{Ave} = -\frac{c_1}{\nu_f - \nu_i} \int_{\nu_i}^{\nu_f} Q_C d\nu \quad (12)$$

where  $c_1$  is a scale factor, and  $\nu$  is the true anomaly of the reference orbit. The metric in Eq. (12) is simply the average of the instantaneous performance over a region of interest. The minus sign is included because we assume that the optimizer will attempt to minimize the function. While this is an intuitive metric, the numerical optimization approach used for this work performed poorly due to numerical reasons. Hence, we formulate a second metric written as

$$J = \int_{\nu_i}^{\nu_f} (3 - Q_{GMS}(L^*)) d\nu \quad (13)$$

This metric is simply the area between the ideal performance and actual performance curves, because according to Eq. (11) the ideal instantaneous performance is always three. When the integral in Eq. (13) is zero, then the performance is ideal over the entire region of interest.

The performance metric defined in Eq. (13) is used to generate all of the solutions presented in this paper. In the next few sections we discuss some remaining issues that must be addressed in order to completely pose the optimization problem. The first is the choice of independent variables. The second is the development of a good initial guess.

## Independent Variables

The choice of independent variables is important in the success of an optimization process and can affect the final solution and the time to reach convergence if using an iterative method. In this section we discuss the parameterization chosen for this work.

There are many possibilities for choosing independent variables for the orbit optimization investigated here. Recall that there are four MMS spacecraft. There are six state variables associated with the orbit state of each spacecraft. In this work we assume Keplerian motion, so the orbit dynamics are not explicit functions of time. Hence, there is a maximum of 24 independent variables for describing the motion. However, we require that the periods of all the orbits must be equal. This is equivalent to the following three constraints

$$\begin{aligned} a_1 &= a_2 \\ a_2 &= a_3 \\ a_3 &= a_4 \end{aligned}$$

where  $a_1$  is the semimajor axis of orbit one and so on. If we choose the independent variables carefully these constraints can be satisfied implicitly. Hence we choose to work with the Keplerian

orbital elements. The vector of independent variables chosen for this work is

$$\mathbf{X} = [a \ e_1 \ i_1 \ \omega_1 \ \Omega_1 \ \nu_1 \ e_2 \ i_2 \ \omega_2 \ \Omega_2 \ \nu_2 \ e_3 \ i_3 \ \omega_3 \ \Omega_3 \ \nu_3 \ e_4 \ i_4 \ \omega_4 \ \Omega_4 \ \nu_4]^T \quad (14)$$

where  $a$  is the semimajor axis of all orbits,  $e$  is the eccentricity,  $i$  is the inclination,  $\omega$  is the argument of periapsis,  $\Omega$  is the right ascension of the ascending node,  $\nu$  is the true anomaly, and the subscripts represent the spacecraft number.

Recall that for phase one, the desired orbit dimensions are  $1.2 \times 12 R_e$ . We must impose additional constraints to ensure that the orbit solutions have dimensions similar to  $1.2 \times 12 R_e$ . In this work we have not tried to meet these constraints exactly. Rather, we wish to characterize the performance possible using orbits with dimensions near  $1.2 \times 12 R_e$ . There are several motivating factors for this work. First, the solutions are computationally demanding and relaxing some constraints is helpful to find solutions efficiently. Secondly, the allowable tolerances on the orbit dimensions have not been specified by the MMS Project. Reasonable constraints to bound the orbit dimensions are

$$1.15 R_e < r_p < 1.31 R_e \quad (15)$$

$$11.82 R_e < r_a < 12.36 R_e \quad (16)$$

where  $R_e$  is the radius of the earth,  $r_a$  is the radius at apogee, and  $r_p$  is the radius at perigee. The upper bound constraints on the independent variable vector,  $\mathbf{X}$ , are given by

$$41905 \text{ km} < a < 43095 \text{ km}$$

$$.80 < e_i < .83$$

$$9.5^\circ < i_i < 10.5^\circ$$

$$85.293^\circ < \omega_i < 95.293^\circ$$

$$-\infty < \Omega_i < \infty$$

$$-\infty < \nu_i < \infty$$

where the subscript  $i$  denotes the spacecraft number.

The last remaining issue to resolve before solving the optimization problem is to develop an algorithm that provides good initial guesses. This is addressed in the next section.

## Initial Guess

Providing a good initial guess is essential to finding optimal solutions and especially when using a method such as SQP that converges to locally optimal solutions. Here we develop an algorithm that provides a good initial guess given a few user-defined parameters. The first parameter is the side length,  $L$ , of the desired tetrahedron. The second parameter is the true anomaly at which we desire the orbit to be in a regular tetrahedron,  $\nu_r$ .

We begin with the orbital elements for the reference orbit and a given value of  $\nu_r$ .

$$\mathbf{oe}_r = [42095.0 \ .818 \ 10^\circ \ 90^\circ \ 0 \ \nu_r]; \quad (17)$$

where the format for  $\mathbf{oe}_r$  is given by  $[a \ e \ i \ \omega \ \Omega \ \nu]$ . Knowing  $\mathbf{oe}_r$  we can find the cartesian state defined by  $\mathbf{r}_r$  and  $\mathbf{v}_r$  using the well known transformation described in Vallado.<sup>3</sup> The energy,  $\mathcal{E}$ , of the reference orbit, as well as the remaining three orbits is given by

$$\mathcal{E} = -\frac{\mu}{2a} \quad (18)$$

For a given value of  $L$ , assumed to be 10 km for this work, we can use Eqs. (1-3) to determine a regular tetrahedron about the reference orbit at  $\nu_r$  using the relations below. For simplicity we denote orbit 1 as the reference orbit.

$$\mathbf{r}_1 = \mathbf{r}_r \quad (19)$$

$$\mathbf{r}_2 = \mathbf{r}_r + \mathbf{d}_1 \quad (20)$$

$$\mathbf{r}_3 = \mathbf{r}_r + \mathbf{d}_2 \quad (21)$$

$$\mathbf{r}_4 = \mathbf{r}_r + \mathbf{d}_3 \quad (22)$$

As an initial guess we assume that the velocities of all four spacecraft are in the same direction as the velocity vector for orbit 1. Hence the velocity direction is

$$\hat{\mathbf{v}} = \frac{\mathbf{v}}{\|\mathbf{v}\|} \quad (23)$$

We now only need to determine the magnitude of the velocity for the last three spacecraft. This is done using the vis-viva equation.

$$v_2 = \sqrt{2(\mathcal{E} + \mu/\|\mathbf{r}_2\|)} \quad (24)$$

$$v_3 = \sqrt{2(\mathcal{E} + \mu/\|\mathbf{r}_3\|)} \quad (25)$$

$$v_4 = \sqrt{2(\mathcal{E} + \mu/\|\mathbf{r}_4\|)} \quad (26)$$

Now that the velocity magnitudes are known, we can write the velocity vectors for all four spacecraft as

$$\mathbf{v}_1 = \mathbf{v}_r \quad (27)$$

$$\mathbf{v}_2 = v_2 \hat{\mathbf{v}} \quad (28)$$

$$\mathbf{v}_3 = v_3 \hat{\mathbf{v}} \quad (29)$$

$$\mathbf{v}_4 = v_4 \hat{\mathbf{v}} \quad (30)$$

With Eqs. (19 - 22) and Eqs. (27 - 30) we know the states of all four orbits and simply need to convert the cartesian states to orbital elements to construct the independent variable vector shown in Eq. (14).

Above we have described an algorithm to generate a regular tetrahedron of side length  $L$  at a desired true anomaly  $\nu_r$  of the reference orbit. In the next section we briefly discuss some details of the numerical optimization routine we use.

## Optimizer

There are numerous choices for numerical optimization routines that are applicable for this work. Because we have bound constraints on the independent variables, we must choose a method that

can handle linear constraints. For this work we have chosen to use SQP. The specific package we have chosen to use is MATLAB's *fmincon* function. For details on the *fmincon* routine, we refer the reader to the documentation for MATLAB's *Optimization Toolbox*.<sup>4</sup> There are no known analytic formulations for the gradient of the performance metric described in Eq. (13) with respect to the independent variables described in Eq. (14). Hence, for this work all of the derivatives are calculated using finite differencing.

To pose an optimization problem we must formulate a performance metric and choose a set of independent variables, often called the parameterization. If using an iterative approach, we must also provide an initial guess. In this section we developed a performance metric that relates the orbital dynamics of the four MMS spacecraft to the science return for the mission. We also developed an algorithm for generating initial guesses for the orbit configuration given the tetrahedron side length and the desired point in the reference orbit where we want a regular tetrahedron to occur. We posed a set of bound constraints to ensure that the optimal solutions have the appropriate dimensions for phase I of the MMS mission. We briefly discussed the numerical optimization software package we have chosen. In the next section we present the results of the optimization process. We discuss several solutions in detail, and then present some general conclusions.

## RESULTS

Several hundred optimal solutions have been determined, and in this section we present two solutions in detail and discuss some general trends seen in all of the solutions. The solutions presented in this section are differentiated by the specific limits used in the optimization process. Recall that the performance metric seen in Eq. (13) is a function of the region of interest defined by  $\nu_i$ , and  $\nu_f$ . The motivation for casting the performance metric with these limits of integration is to allow us to determine which parts of the orbit we can provide the best performance, and allow us to determine which portions of the orbit will inevitably result in poor science return.

### Detailed Results

In the following section we discuss a few solutions in detail. The difference between the solutions are the limits of integration,  $\nu_i$ , and  $\nu_f$ , used in Eq. (13). The intention in presenting a few solutions in detail is to provide an intuitive understanding of the relative motion characteristics of different optimal solutions.

In Figure 2 we see plots that describe the characteristics of the optimal solution for  $\nu_i = 160$  and  $\nu_f = 200$ . See table 1 in the Appendix for the orbit state information. The vertical lines in the plots bound the region of interest for the particular solution. The top plot shows the instantaneous performance of the tetrahedron. Recall that the maximum possible performance value at any given instant is three. The two curves in the top plot show the evolution of  $Q_C$  and  $Q_{GM}$  over one orbit. Recall that  $Q_C$  penalizes a solution when the average side length,  $L^*$ , is less than 4 km, and greater than 18 km.  $Q_C$  is shown by the solid line. The Glassmeier performance metric,  $Q_{GM}$ , is shown by the dotted line. Note both curves were generated using the same orbital states. The only difference in the two curves is the performance metric. The dotted curve gives information about the shape of the formation only. The solid curve gives information about both the size and the shape. The middle plot in Figure 2 shows the lengths of all six sides of the tetrahedron over one complete orbit.

The bottom plot shows the average side length over one complete orbit.

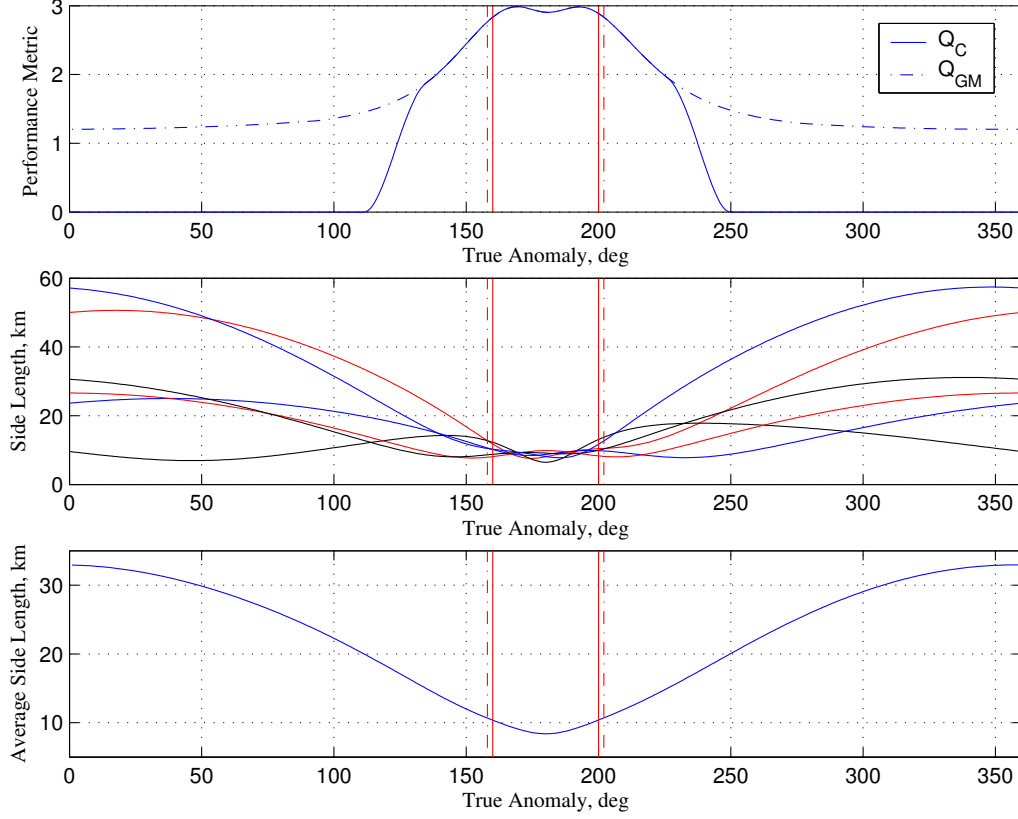


**Figure 2:** Point Solution One

Examining the top plot in Figure 2, we see that during the region of interest the performance is excellent. The average over the region of interest is 2.94. The performance between  $\nu_i = 160$  and  $\nu_f = 200$  comes at the expense of poor performance outside of the region of interest. From this plot we learn that it is possible to provide excellent performance at orbit apogee for at least  $\pm 20^\circ$ . Notice in the second plot in Figure 2 that the side lengths are all near 10 km during the region of interest. Outside the region of interest the side lengths vary between 10 and 60 km. These variations in the side lengths are acceptable according to current design requirements for maximum and minimum inter-spacecraft separations.

Another optimal solution is shown in Figure 3. The region of interest for this solution is between  $\nu_i = 45$  and  $\nu_f = 135$ . The states for this solution are found in table 2 in the Appendix. This solution was presented to illustrate the performance of tetrahedrons optimized in regions not centered on apogee. We see that during the region of interest the performance is excellent and the average is 2.95. As in the previous solution, the performance between  $\nu_i = 160$  and  $\nu_f = 200$  comes at the expense of poor performance outside of the region of interest. We see that it is possible to provide excellent performance for up to at least a  $90^\circ$  band in true anomaly, for off-apogee regions of interest. The second plot in Figure 3 shows that the side lengths are all near 10 km during the region of interest. Notice that at about  $\nu = 145^\circ$  the lengths of one of the sides of the tetrahedron is only about 2 km. This may cause some difficulties and may require some slight redesign once

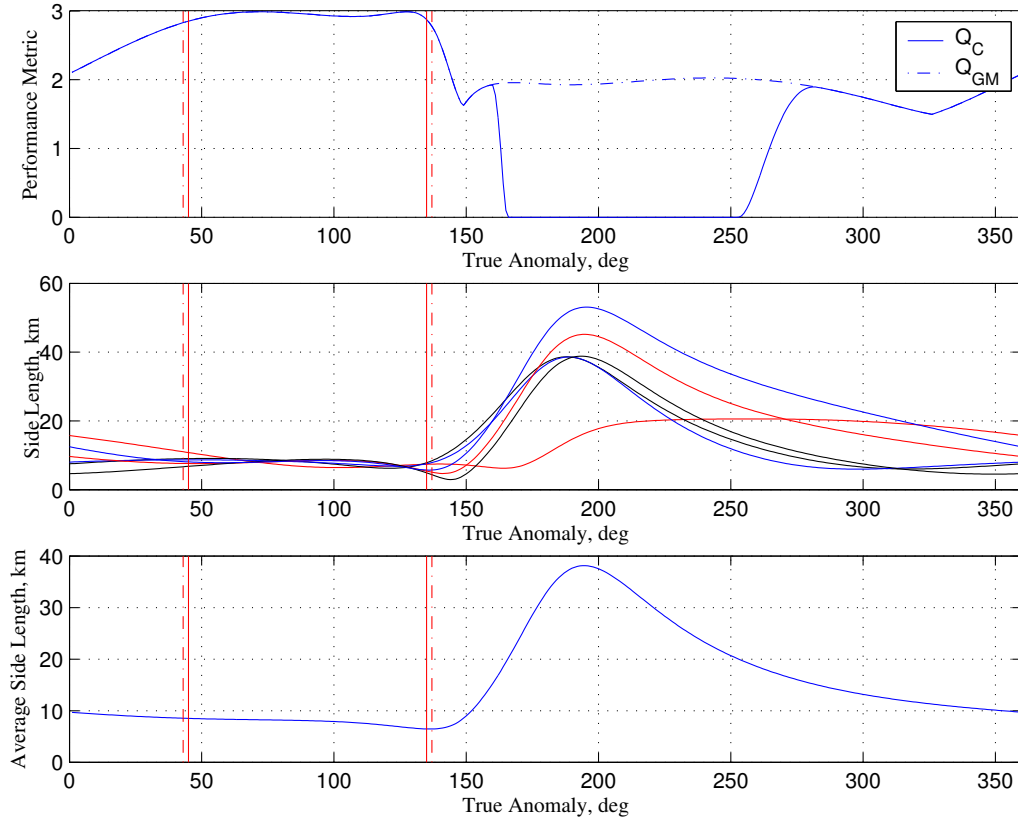


**Figure 3:** Point Solution Two

collision avoidance requirements are finalized. The maximum side length that occurs is about 55 km and is acceptable given current baseline requirements on maximum separation distances.

While the two solutions discussed in detail here both demonstrate that we can provide excellent performance over significant portions of the orbit, it is not in general possible to provide near ideal performance for the entire orbit. In fact there are regions of the orbit where it is more difficult to maintain regular tetrahedrons. Also, in different portions of the orbit it is possible to maintain regular tetrahedrons for longer periods of time compared to other orbit regions. In the next section we discuss some general trends and determine orbital regions where we can provide the best performance.

## General Results and Trends

We demonstrated in the previous section that it is possible to provide near ideal performance for significant portions of the orbit. In this section we draw some general conclusions about where in the orbit the best performance can be provided, and for how long.

To aid in the understanding of the results, we employ a simple change of variables described below

$$\nu_c = (\nu_f + \nu_i)/2 \quad (31)$$

$$\Delta\nu = \nu_f - \nu_i \quad (32)$$

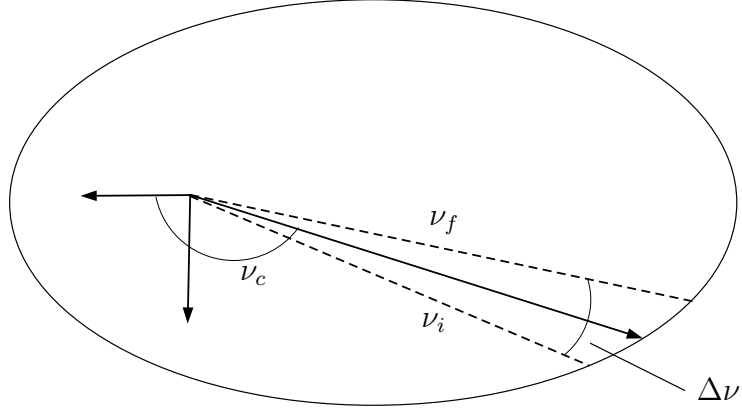


**Figure 4:** Definition of  $\nu_c$  and  $\Delta\nu$

A graphical description of the relationships between  $\nu_c$  and  $\Delta\nu$  and  $\nu_i$  and  $\nu_f$  is shown in Figure 4. We have systematically chosen sets of  $\nu_c$  and  $\Delta\nu$  and found optimal solutions to the performance metric shown in Eq. (13) for each pair. We have picked 324 combinations of  $\nu_c$  and  $\Delta\nu$  defined as follows.  $\nu_c$  is varied from  $90^\circ$  to  $270^\circ$  in increments of  $10^\circ$ . For each value of  $\nu_c$  we vary  $\Delta\nu$  from  $10^\circ$  to  $180^\circ$  in increments of  $10^\circ$ .

A contour plot of the optimal average performance vs  $\nu_c$  and  $\Delta\nu$  is shown in Figure 5. The average performance is defined as the average of the instantaneous performance metric, of the optimized tetrahedron, over the region defined by  $\nu_c$  and  $\Delta\nu$ . Upon inspection of Figure 5 we see that for regions of  $\Delta\nu < 40^\circ$  we can provide average performance levels of 2.95 or better. Recall that the ideal performance according to Eq. (13) is 3.0. Hence we can provide near ideal performance for  $\Delta\nu \leq 40^\circ$  regardless of the value of  $\nu_c$ .

In general, the ability to maintain near ideal performance for long durations degrades as  $\nu_c$  moves towards apogee. As an example, for  $\nu_c = 180^\circ$  and  $\Delta\nu = 100^\circ$  we can provide an average performance of about 2.75. However, for  $\nu_c = 90^\circ$  and  $\Delta\nu = 100^\circ$  we can provide an average performance of about 2.9. An even more pronounced example occurs at  $\nu_c = 90$  and  $\Delta\nu = 140^\circ$ . In this case we can provide an average performance of 2.8 for a large portion of the orbit. Another general trend in the performance is that it tends to degrade as  $\Delta\nu$  increases. For  $\Delta\nu = 180^\circ$  we can only provide average performance levels of around 2.65. The regions of poorest performance occur at a value of 2.5. These regions occur near  $\Delta\nu = 160$  for values of  $\nu_c$  of about 160 and 200.

From the contour plot seen in Figure 5 we see that we can provide excellent performance over large portions of the orbit. However, there are regions of the orbit where it is more difficult to maintain near ideal performance for long durations. In the next section we provide a summary of the approach used in this paper, and summarize our results.

## CONCLUSIONS

In this work we solved for initial conditions that provide optimal formation configurations for phase I of the MMS mission. Ideally, the formation should maintain a regular tetrahedron over the entire orbit. However, this is not possible under Keplerian motion alone. Hence, the goal of this work was

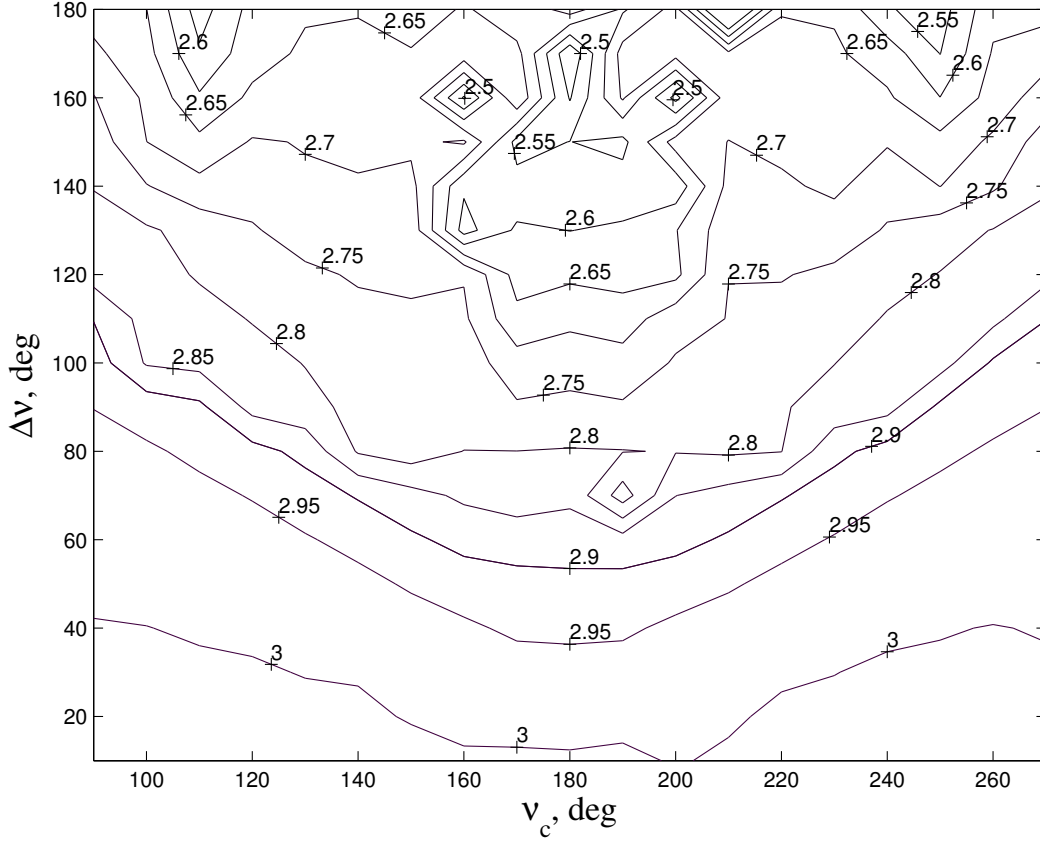


**Figure 5:** Contour Plot of Formation Performance vs.  $\nu_c$  and  $\Delta\nu$

to find the best possible tetrahedron configurations, and identify which portions of the orbit we can provide near ideal performance for the longest duration.

We began by discussing some basic properties of tetrahedrons such as the volume and surface area. These basic properties were used to develop a performance metric that reflects both the quality of the tetrahedron shape, as well as the size of the tetrahedron. The performance metric used in this work was a modification of work previously performed by Glassmeier.<sup>2</sup> We also developed an initial guess algorithm that allows a user to construct a formation of spacecraft in a regular tetrahedron configuration about a defined location in the reference orbit.

Several hundred optimal formations were found by considering different regions of interest in the orbit. We presented two solutions in detail to demonstrate that near ideal performance can be provided for large regions of interest. At apogee, we can provide average performance levels of 2.9, where 3.0 is the maximum, for up to 40 degrees in true anomaly. At off apogee positions it is easier to provide near ideal performance. For a region bounded by a lower true anomaly of  $45^\circ$  and an upper true anomaly of  $135^\circ$ , it is possible to provide an average performance of 2.95. Hence in general it is more difficult to provide high average performance for large spans of true anomaly near apogee. There is also a downward trend as the span of true anomaly increases.

## REFERENCES

- [1] S. Curtis, “The Magnetospheric Multiscale Mission...Resolving Fundamental Processes in Space Plasmas,” *NASA Technical Memorandum*, NASA/GSFC, 2000.
- [2] G. Paschmann and P. W. Daly, “Analysis Methods for Multi-Spacecraft Data”, ESA Publications Division, Netherlands, 1998.
- [3] D.A. Vallado, “Fundamentals of Astrodynamics and Applications, 2nd Edition”, Kluwer Academic Publishers, Dordrecht, 2001.
- [4] *Optimization Toolbox User’s Guide*. The Mathworks, Jan 1999.

## APPENDIX

**Table 1:** States Associated with Figure 2

State Variable	Orbit One	Orbit Two	Orbit Three	Orbit Four
$a$ (km)	42256.691	42256.691	42256.691	42256.691
$e$	0.80229	0.80221	0.80214	0.80220
$i$ (deg.)	10.0481	10.0493	10.0486	10.0426
$\omega$ (deg.)	90.2462	90.2623	90.2540	90.2591
$\Omega$ (deg.)	-0.06204	-0.06873	-0.07096	-0.07084
$\nu$ (deg.)	180.1627	180.1585	180.1634	180.1608

**Table 2:** States Associated with Figure 3

State Variable	Orbit One	Orbit Two	Orbit Three	Orbit Four
$a$ (km)	42102.032 km	42102.032 km	42102.032 km	42102.032 km
$e$	0.81776	0.81788	0.81766	0.8177
$i$ (deg.)	9.9805	9.9841	9.9802	10.0023
$\omega$ (deg.)	90.0877	90.1032	90.1447	89.9559
$\Omega$ (deg.)	0.0332	0.0131	0.0041	0.1843
$\nu$ (deg.)	90.0123	90.0236	89.9572	89.9865